



# CHORUS

This is the accepted manuscript made available via CHORUS. The article has been published as:

## In-medium nucleon-nucleon cross sections with nonspherical Pauli blocking

L. White and F. Sammarruca

Phys. Rev. C **90**, 044607 — Published 15 October 2014

DOI: [10.1103/PhysRevC.90.044607](https://doi.org/10.1103/PhysRevC.90.044607)

# In-medium nucleon-nucleon cross-sections with non-spherical Pauli blocking

L. White\* and F. Sammarruca†

*Physics Department, University of Idaho, Moscow, ID 83844-0903, U.S.A*

(Dated: September 29, 2014)

We present a formalism to solve the Bethe-Goldstone scattering equation without the use of partial wave expansion which is alternative to the one we developed in a previous work. The present approach is more suitable for the calculation of in-medium nucleon-nucleon cross sections, which are the focal point of this paper. The impact of removing the spherical approximation on the angle and energy dependence of, particularly, in-medium proton-proton and proton-neutron differential cross sections is discussed along with its potential implication.

## I. INTRODUCTION

The Bethe-Goldstone equation [1–4] describes nucleon-nucleon (NN) scattering in a dense hadronic medium. Conventional medium effects present in the equation include corrections of the single-particle energies to account for the presence of the medium and the Pauli blocking mechanism, which prevents scattering into occupied states. Within the Dirac-Brueckner-Hartree-Fock (DBHF) approach, which is our traditional framework, an additional “non conventional” medium effect comes in through the use of the (density-dependent) nucleon effective mass in the nucleon Dirac spinors.

In a previous work [5], we presented a method for the solution of the Bethe-Goldstone equation without the use of partial wave decomposition in order to remove the spherical, or angle average, approximation on the Pauli blocking operator. With that as our baseline, in this paper we consider the idealized scenario of two nucleons undergoing scattering in infinite, symmetric or asymmetric, nuclear matter, and calculate in-medium cross sections for such a process, using as input a G-matrix obtained from the solution of the Bethe-Goldstone equation in three-dimensional space. A crucial step for accomplishing such solution in a manageable way is the removal of the azimuthal degree of freedom from the starting three-dimensional equation. First, we will describe why we need to take a different approach than the one we adopted in Ref. [5] if we wish to place the incident momentum along the direction of the chosen quantization axis, the  $z$ -axis, as typically done in standard calculations of NN observables. As a consequence of that, we will propose an alternative method to partially decouple the system of (helicity basis) equations. These and other technical issues (if significantly different than those previously reported), will be confronted in Section II.

After incorporating (non-spherical) Pauli blocking and other appropriate medium effects, we proceed to calculate in-medium differential cross sections. Clearly in-medium scattering (that is, the scattering of two nucleons embedded in nuclear matter), is not a directly observable process. A connection with physical scattering can be made considering, for instance, a nucleon bound in a nucleus (or, more ideally, in nuclear matter, as in our case) through the nuclear mean field. If such nucleon is struck [for instance, as in a  $(e, e')$  reaction], it may subsequently scatter from another nucleon. This process would require the knowledge of the in-medium NN cross-section, or *effective* cross-section.

Another scenario which involves in-medium two-body cross-sections is the dynamics of heavy-ion collisions. These are typically handled with so-called transport equations, such as the Boltzmann-Uehling-Uhlenbeck equation [6, 7], which describe the evolution of a system of strongly interacting hadrons drifting in the presence of a mean field while undergoing two-body collisions.

In-medium cross-sections are driven by the scattering amplitudes as well as kinematical factors. In a microscopic approach, they are constructed from the (medium-modified) NN amplitudes without phenomenology. They depend on several variables, such as the relative momentum of the two-nucleon pair, the total momentum of the pair in the nuclear matter rest frame (needed for the Pauli operator), and, potentially, two different densities or Fermi momenta. To facilitate applications in reactions, these multiple dependences have been handled in different ways and with different levels of approximations. In the simplest approach, the assumption is made that the transition matrix in the medium is approximately the same as in vacuum, and that medium effects on the cross-section come in only through the use of nucleon effective masses in the phase space factors [8–10]. Concerning microscopic approaches, some can be found, for instance, in Refs. [11–13], but consideration of medium asymmetries are not included in those predictions. Furthermore, in Refs. [11, 12], the full (complex) nature of the scattering amplitude is not taken into account, and in-

---

\* Email:whitel20ster@gmail.com

† Email:fsammarr@uidaho.edu

medium differential cross sections are calculated from a (real)  $K$ -matrix. Finally, all previous microscopic predictions make use of the angle-averaged Pauli operator.

Effective cross-sections can also provide information on the nucleon mean-free path in nuclear matter, a quantity of fundamental importance to understand the dynamics of a nucleon in the medium. In summary, they are an important input for several processes. It is one of the goals of this paper to investigate to which extent our microscopic in-medium observables are sensitive to the exact treatment of Pauli blocking, and, more generally, to examine how their angular structure and energy dependence are impacted by the medium.

Our results are presented and discussed in Sec. III, while Sec. IV contains a short summary and our conclusions.

## II. FORMAL ASPECTS

### A. Free space: the Thompson equation in a helicity basis

As we did previously, we start with the (free-space) Thompson equation in a helicity. More explicitly, the Thompson equation which we adopt is given as [5]

$$\langle \lambda'_1 \lambda'_2 | \hat{T}^I(\mathbf{q}', \mathbf{q}) | \lambda_1 \lambda_2 \rangle = \langle \lambda'_1 \lambda'_2 | \hat{V}^I(\mathbf{q}', \mathbf{q}) | \lambda_1 \lambda_2 \rangle + \sum_{\lambda''_1, \lambda''_2 = \pm} \int_{\mathbb{R}^3} \frac{\langle \lambda'_1 \lambda'_2 | \hat{V}^I(\mathbf{q}', \mathbf{q}'') | \lambda''_1 \lambda''_2 \rangle \langle \lambda''_1 \lambda''_2 | \hat{T}^I(\mathbf{q}'', \mathbf{q}) | \lambda_1 \lambda_2 \rangle}{2(E_q - E_{q''} + i\epsilon)} d^3 q'' . \quad (1)$$

Above  $\hat{T}$ ,  $\hat{V}$ ,  $I$ ,  $E_p = \sqrt{p^2 + m^2}$  and  $m$  are the  $T$ -matrix, NN potential (see Appx. A of Ref. [5]), total isospin, relativistic energy, and nucleon mass (average of the proton and neutron mass) respectively. Furthermore,  $\mathbf{q}$ ,  $\mathbf{q}'$ , and  $\mathbf{q}''$  are the initial, final, and intermediate momenta in the two-nucleon center-of-mass frame.

The first issue to be addressed is the removal of the azimuthal degree of freedom, which can be done in a number of ways. The average over the azimuthal angle performed as in Eqs. (7a-b) of Ref. [5] in the spirit of Ref. [14] causes some of the matrix elements to vanish if the initial momentum is along the  $z$ -axis (i.e.  $\theta = 0$ ), therefore here we will adopt a different prescription. Placing the initial momentum along the  $z$ -axis, we observe the resulting symmetry of the NN potential:

$$\langle \lambda'_1 \lambda'_2 | \hat{V}^I(\mathbf{q}', q, 0, \phi) | \lambda_1 \lambda_2 \rangle = e^{i\Lambda(\phi' - \phi)} \langle \lambda'_1 \lambda'_2 | \hat{V}^I(\tilde{q}', 0, q, 0, 0) | \lambda_1 \lambda_2 \rangle \equiv e^{i\Lambda(\phi' - \phi)} \langle \lambda'_1 \lambda'_2 | v^I(\tilde{q}', q) | \lambda_1 \lambda_2 \rangle , \quad (2)$$

with  $\Lambda \equiv \lambda_1 - \lambda_2$  and  $\tilde{q}' \equiv (q', \theta')$ . This symmetry, which carries over to the  $T$ -matrix, can easily be shown by writing the  $T$ -matrix (and NN potential) in a partial wave helicity basis expansion [see Eq. (14)].

After setting  $\theta = 0$  in Eq. (1) and implementing the previous observation, in the spirit of Ref. [15] we apply on both side of the equation the operator  $\frac{1}{2\pi} \int_0^{2\pi} e^{-i\Lambda(\phi' - \phi)} d\phi'$  and arrive at the  $\phi$ -integrated Thompson equation

$$\begin{aligned} \langle \lambda'_1 \lambda'_2 | t^I(\tilde{q}', q) | \lambda_1 \lambda_2 \rangle &= \langle \lambda'_1 \lambda'_2 | v^I(\tilde{q}', q) | \lambda_1 \lambda_2 \rangle \\ &+ \sum_{\lambda''_1, \lambda''_2 = \pm} \pi \int_0^\infty \int_0^\pi \frac{\langle \lambda'_1 \lambda'_2 | v^{\Lambda I}(\tilde{q}', \tilde{q}'') | \lambda''_1 \lambda''_2 \rangle \langle \lambda''_1 \lambda''_2 | t^I(\tilde{q}'', q) | \lambda_1 \lambda_2 \rangle}{E_q - E_{q''} + i\epsilon} q''^2 \sin \theta'' d\theta'' dq'' , \end{aligned} \quad (3)$$

with the *real*  $\phi$ -integrated potential equal to

$$\langle \lambda'_1 \lambda'_2 | v^{\Lambda I}(\tilde{q}', \tilde{q}'') | \lambda''_1 \lambda''_2 \rangle = \frac{1}{2\pi} \int_0^{2\pi} e^{i\Lambda(\phi'' - \phi')} \langle \lambda'_1 \lambda'_2 | \hat{V}^I(\mathbf{q}', \mathbf{q}'') | \lambda''_1 \lambda''_2 \rangle |_{\phi'=0} d\phi'' . \quad (4)$$

Note that the  $\phi$ -integrated potential depends on double, single, and unprimed helicities, rendering the present set of equations different than Eq. (8) of Ref. [5]. This calls for a different strategy to partially decouple the system.

### B. Partially decoupling the system of integral equations

The  $\phi$ -integrated Thompson equations are a set of sixteen coupled Fredholm integral equations of the second kind for each isospin. Due to parity and isospin conservation, only six amplitudes are independent. For the six independent amplitudes we choose [5]

$$\begin{aligned} t_1^I &\equiv \langle ++ | t^I | ++ \rangle , & t_2^I &\equiv \langle ++ | t^I | -- \rangle , & t_3^I &\equiv \langle +- | t^I | +- \rangle , \\ t_4^I &\equiv \langle +- | t^I | -+ \rangle , & t_5^I &\equiv \langle ++ | t^I | +- \rangle , & t_6^I &\equiv \langle +- | t^I | ++ \rangle . \end{aligned} \quad (5)$$

Additionally, we found that the following linear combinations

$${}^0t^I \equiv t_1^I - t_2^I, \quad {}^{12}t^I \equiv t_1^I + t_2^I, \quad (6)$$

will partially decouple the system for the  $t_1^I$  and  $t_2^I$  amplitudes.

The symmetries on the  $\phi$ -integrated potential can be found analytically (for instance using a partial wave helicity basis expansion [see Eq. (14)], or numerically. Either way, we end up with the following conclusions: 1) When  $\Lambda = 0$  the symmetries of the  $\phi$ -integrated potential are the same as the corresponding ones for the  $t$ -matrix, see Eq. (9) of Ref. [5]. 2) When  $\Lambda = \pm 1$  the following holds

$$\begin{aligned} v_1^{1I} &\equiv \langle ++ | v^{1I} | ++ \rangle = \langle ++ | v^{-1I} | ++ \rangle = \langle -- | v^{1I} | -- \rangle = \langle -- | v^{-1I} | -- \rangle, \\ v_2^{1I} &\equiv \langle ++ | v^{1I} | -- \rangle = \langle ++ | v^{-1I} | -- \rangle = \langle -- | v^{1I} | ++ \rangle = \langle -- | v^{-1I} | ++ \rangle, \\ v_3^{1I} &\equiv \langle +- | v^{1I} | +- \rangle = \langle +- | v^{-1I} | +- \rangle, \\ v_3^{-1I} &\equiv \langle +- | v^{-1I} | +- \rangle = \langle +- | v^{1I} | +- \rangle, \\ v_4^{1I} &\equiv \langle +- | v^{1I} | -+ \rangle = \langle +- | v^{-1I} | -+ \rangle, \\ v_4^{-1I} &\equiv \langle +- | v^{-1I} | -+ \rangle = \langle +- | v^{1I} | -+ \rangle, \\ v_5^{1I} &\equiv \langle ++ | v^{1I} | +- \rangle = -\langle ++ | v^{-1I} | +- \rangle = \langle -- | v^{1I} | +- \rangle = -\langle -- | v^{-1I} | +- \rangle, \\ v_5^{-1I} &\equiv \langle ++ | v^{-1I} | +- \rangle = -\langle ++ | v^{1I} | +- \rangle = -\langle -- | v^{1I} | +- \rangle = \langle -- | v^{-1I} | +- \rangle, \\ v_6^{1I} &\equiv \langle +- | v^{1I} | ++ \rangle = -\langle +- | v^{-1I} | ++ \rangle = \langle +- | v^{1I} | -- \rangle = -\langle +- | v^{-1I} | -- \rangle, \\ v_6^{-1I} &\equiv \langle +- | v^{-1I} | ++ \rangle = -\langle +- | v^{1I} | ++ \rangle = -\langle +- | v^{1I} | -- \rangle = \langle +- | v^{-1I} | -- \rangle. \end{aligned} \quad (7)$$

If we utilize Eqs. (3) and (5) to (7) along with the symmetries of the  $t$ -matrix (see Eq. 9 in Ref. [5]) we obtain the following six partially coupled integral equations.

The spin singlet amplitude  ${}^0t^I$  is uncoupled

$${}^0t^I(\tilde{q}', q) = {}^0v^I(\tilde{q}', q) + \pi \int_0^\infty \int_0^\pi \frac{{}^0v^{0I}(\tilde{q}', \tilde{q}'') {}^0t^I(\tilde{q}'', q)}{E_q - E_q'' + i\epsilon} q''^2 \sin \theta'' d\theta'' dq''. \quad (8)$$

The spin triplet amplitudes  ${}^{12}t^I$  and  ${}^{66}t^I$  form a bi-coupled system

$${}^{12}t^I(\tilde{q}', q) = {}^{12}v^I(\tilde{q}', q) + \pi \int_0^\infty \int_0^\pi \frac{{}^{12}v^{0I}(\tilde{q}', \tilde{q}'') {}^{12}t^I(\tilde{q}'', q) + 4v_5^{0I}(\tilde{q}', \tilde{q}'') t_6^I(\tilde{q}'', q)}{E_q - E_q'' + i\epsilon} q''^2 \sin \theta'' d\theta'' dq'', \quad (9)$$

$$t_6^I(\tilde{q}', q) = v_6^I(\tilde{q}', q) + \pi \int_0^\infty \int_0^\pi \frac{v_6^{0I}(\tilde{q}', \tilde{q}'') {}^{12}t^I(\tilde{q}'', q) + [v_3^{0I}(\tilde{q}', \tilde{q}'') - v_4^{0I}(\tilde{q}', \tilde{q}'')] t_6^I(\tilde{q}'', q)}{E_q - E_q'' + i\epsilon} q''^2 \sin \theta'' d\theta'' dq''. \quad (10)$$

Finally, the  $t_3^I$ ,  $t_4^I$ , and  $t_5^I$  amplitudes form a tri-coupled system

$$t_3^I(\tilde{q}', q) = v_3^I(\tilde{q}', q) + \pi \int_0^\infty \int_0^\pi \frac{v_3^{1I}(\tilde{q}', \tilde{q}'') t_3^I(\tilde{q}'', q) + v_4^{1I}(\tilde{q}', \tilde{q}'') t_4^I(\tilde{q}'', q) + 2v_6^{1I}(\tilde{q}', \tilde{q}'') t_5^I(\tilde{q}'', q)}{E_q - E_q'' + i\epsilon} q''^2 \sin \theta'' d\theta'' dq'', \quad (11)$$

$$t_4^I(\tilde{q}', q) = v_4^I(\tilde{q}', q) + \pi \int_0^\infty \int_0^\pi \frac{v_4^{-1I}(\tilde{q}', \tilde{q}'') t_3^I(\tilde{q}'', q) + v_3^{-1I}(\tilde{q}', \tilde{q}'') t_4^I(\tilde{q}'', q) - 2v_6^{-1I}(\tilde{q}', \tilde{q}'') t_5^I(\tilde{q}'', q)}{E_q - E_q'' + i\epsilon} q''^2 \sin \theta'' d\theta'' dq'', \quad (12)$$

$$t_5^I(\tilde{q}', q) = v_5^I(\tilde{q}', q) + \pi \int_0^\infty \int_0^\pi \frac{v_5^{1I}(\tilde{q}', \tilde{q}'') t_3^I(\tilde{q}'', q) - v_5^{-1I}(\tilde{q}', \tilde{q}'') t_4^I(\tilde{q}'', q) + {}^{12}v^{1I}(\tilde{q}', \tilde{q}'') t_5^I(\tilde{q}'', q)}{E_q - E_q'' + i\epsilon} q''^2 \sin \theta'' d\theta'' dq''. \quad (13)$$

Concerning the numerical solution, the strategies shown in Appx. B of Ref. [5] can be easily adapted to this particular set of equations.

### C. Connection with partial wave decomposition and construction of NN observables

Although the point of this paper is to avoid the method of partial-wave expansion, we utilize the partial wave solution for comparison purposes. The expansion of  $\hat{T}^I(\mathbf{q}', \mathbf{q})$  in a partial wave helicity basis [16, 17] is given by

$$\langle \lambda'_1 \lambda'_2 | \hat{T}^I(\mathbf{q}', \mathbf{q}) | \lambda_1 \lambda_2 \rangle = \sum_{JM} \frac{2J+1}{4\pi} D_{M\Lambda'}^J(\phi', \theta', -\phi')^* \langle \lambda'_1 \lambda'_2 | \hat{T}^{IJ}(q', q) | \lambda_1 \lambda_2 \rangle D_{M\Lambda}^J(\phi, \theta, -\phi), \quad (14)$$

where the Wigner  $D$ -matrix  $D_{M\Lambda}^J(\alpha, \beta, \gamma) = e^{-iM\alpha} d_{M\Lambda}^J(\beta) e^{-i\Lambda\gamma}$  includes the reduced rotation matrix  $d_{M\Lambda}^J(\beta)$  with  $\Lambda \equiv \lambda_1 - \lambda_2$  and an analogous definition for the primed coordinate. The partial wave amplitudes, denoted by  $\hat{T}^{IJ}(q', q)$  (with a similar decomposition done for the NN potential), are the solutions of the partial wave decomposed Eq. (1).

To obtain a transformation from partial waves into the (angle-dependent)  $t$ -matrix we evaluate Eq. (14) at  $\phi' = \theta = \phi = 0$

$$\langle \lambda'_1 \lambda'_2 | t^I(\tilde{q}', q) | \lambda_1 \lambda_2 \rangle = \sum_J \frac{2J+1}{4\pi} d_{\Lambda\Lambda'}^J(\theta') \langle \lambda'_1 \lambda'_2 | \hat{T}^{IJ}(q', q) | \lambda_1 \lambda_2 \rangle. \quad (15)$$

As it stands, our angle-dependent solutions contain unphysical states. On the other hand, the well-known antisymmetry requirement for the NN system imply that only even or odd values of  $J$  are allowed in a particular state of definite spin and isospin. Thus, starting with Eq. (15) and making use of the identities  $(-1)^J d_{00}^J(\theta') = d_{00}^J(\pi - \theta')$ ,  $(-1)^{J+1} d_{01}^J(\theta') = d_{01}^J(\pi - \theta')$ ,  $(-1)^J d_{11}^J(\theta') = -d_{-11}^J(\pi - \theta')$ , and  $(-1)^J d_{-11}^J(\theta') = -d_{11}^J(\pi - \theta')$  we can, in each case, identify the appropriate combination of the direct and the exchange terms which must enter the antisymmetrized amplitudes. For those, we obtain:

$${}^0t_a^{\dot{0}}(\tilde{q}', q) \equiv \frac{1}{2} [{}^0t^{\dot{0}}(\tilde{q}', q) \pm {}^0t^{\dot{0}}(-\tilde{q}', q)] = \sum_{J=\text{even}} \frac{2J+1}{4\pi} d_{00}^J(\theta') {}^0T^{J\dot{0}}(q', q), \quad (16)$$

$${}^{12}t_a^{\dot{0}}(\tilde{q}', q) \equiv \frac{1}{2} [{}^{12}t^{\dot{0}}(\tilde{q}', q) \pm {}^{12}t^{\dot{0}}(-\tilde{q}', q)] = \sum_{J=\text{even}} \frac{2J+1}{4\pi} d_{00}^J(\theta') {}^{12}T^{J\dot{0}}(q', q), \quad (17)$$

with,

$$t_{a,1}^{\dot{0}}(\tilde{q}', q) = \frac{1}{2} [{}^{12}t_a^{\dot{0}}(\tilde{q}', q) + {}^0t_a^{\dot{0}}(\tilde{q}', q)] \quad \text{and} \quad t_{a,2}^{\dot{0}}(\tilde{q}', q) = \frac{1}{2} [{}^{12}t_a^{\dot{0}}(\tilde{q}', q) - {}^0t_a^{\dot{0}}(\tilde{q}', q)], \quad (18)$$

$$t_{a,6}^{\dot{0}}(\tilde{q}', q) \equiv \frac{1}{2} [t_6^{\dot{0}}(\tilde{q}', q) \mp t_6^{\dot{0}}(-\tilde{q}', q)] = \frac{1}{2} \sum_{J=\text{even}} \frac{2J+1}{4\pi} d_{01}^J(\theta') {}^{66}T^{J\dot{0}}(q', q), \quad (19)$$

$$t_{a,3}^{\dot{0}}(\tilde{q}', q) \equiv \frac{1}{2} [t_3^{\dot{0}}(\tilde{q}', q) \mp t_4^{\dot{0}}(-\tilde{q}', q)] = \frac{1}{2} \left[ \sum_{J=\text{even}} \frac{2J+1}{4\pi} d_{11}^J(\theta') {}^{34}T^{J\dot{0}}(q', q) + \sum_{J=\text{odd}} \frac{2J+1}{4\pi} d_{11}^J(\theta') {}^1T^{J\dot{0}}(q', q) \right], \quad (20)$$

$$t_{a,4}^{\dot{0}}(\tilde{q}', q) \equiv \frac{1}{2} [t_4^{\dot{0}}(\tilde{q}', q) \mp t_3^{\dot{0}}(-\tilde{q}', q)] = \frac{1}{2} \left[ \sum_{J=\text{even}} \frac{2J+1}{4\pi} d_{-11}^J(\theta') {}^{34}T^{J\dot{0}}(q', q) - \sum_{J=\text{odd}} \frac{2J+1}{4\pi} d_{-11}^J(\theta') {}^1T^{J\dot{0}}(q', q) \right], \quad (21)$$

$$t_{a,5}^{\dot{0}}(\tilde{q}', q) \equiv \frac{1}{2} [t_5^{\dot{0}}(\tilde{q}', q) \mp t_5^{\dot{0}}(-\tilde{q}', q)] = \frac{1}{2} \sum_{J=\text{even}} \frac{2J+1}{4\pi} d_{10}^J(\theta') {}^{55}T^{J\dot{0}}(q', q), \quad (22)$$

where definitions for the linear combinations of partial wave amplitudes  ${}^n T^{J0}$ ,  $n = 0, 1, 12, 34, 55, 66$  are given in Ref. [18]. Also, above one must read across the top (or bottom) to associate the correct sign with the appropriate  $J$  values (even or odd) and isospin (0 or 1). We also used the shorthand notation for the exchange amplitude  $t^I(-\tilde{q}', \tilde{q}) = t^I(q', \pi - \theta', q, \theta)$ .

We are now in a position to calculate in-medium observables as functions of the scattering angle relative to the  $z$ -axis, for which purpose we will use the Hoshizaki spin formalism [19]. We will calculate the elastic differential cross-section,  $\frac{d\sigma}{d\Omega}$ , and a representative spin observable, for which we choose the depolarization  $D$  (also denoted as  $D_{nn}$ ). The latter refers to an experiment where beam and target are polarized in the direction normal to the scattering plane.

First, as in Table VII of Ref. [19], we define

$$4a = \varphi_1 - \varphi_2 + \varphi_3 + \varphi_4 + (\varphi_1 + \varphi_2 + \varphi_3 - \varphi_4) \cos \theta_{cm} - 4\varphi_5 \sin \theta_{cm} , \quad (23)$$

$$4ic = (\varphi_1 + \varphi_2 + \varphi_3 - \varphi_4) \sin \theta_{cm} + 4\varphi_5 \cos \theta_{cm} , \quad (24)$$

$$4m = -\varphi_1 + \varphi_2 - \varphi_3 - \varphi_4 + (\varphi_1 + \varphi_2 + \varphi_3 - \varphi_4) \cos \theta_{cm} - 4\varphi_5 \sin \theta_{cm} , \quad (25)$$

$$4g = -\varphi_1 + \varphi_2 + \varphi_3 + \varphi_4 , \quad (26)$$

$$4h = -\varphi_1 - \varphi_2 + \varphi_3 - \varphi_4 , \quad (27)$$

where the Hoshizaki  $\varphi_n$  amplitudes are related to our  $t_n$  as

$$\varphi_n(q, \theta_{cm}) = (2\pi)^2 \frac{E}{2} t_n(q, \theta_{cm}, q) \quad \text{for } n = 1, 2, 3, 4, 5, \quad \text{with } E = \sqrt{m^2 + q^2}, \quad (28)$$

and

$$t_n(q', \theta', q) = \begin{cases} t_{a,n}^0(q', \theta', q) + t_{a,n}^1(q', \theta', q) & np \text{ observables} \\ 2t_{a,n}^1(q', \theta', q) & pp \text{ observables.} \end{cases} \quad (29)$$

In terms of the Hoshizaki amplitudes  $a, c, m, g$ , and  $h$ , we have (as in Table I of Ref. [19])

$$\frac{d\sigma}{d\Omega} = |a|^2 + |m|^2 + 2(|c|^2 + |g|^2 + |h|^2) , \quad (30)$$

$$\frac{d\sigma}{d\Omega} (1 - D) = 4(|g|^2 + |h|^2) . \quad (31)$$

We can write Eq. [30] in an alternative way, which best shows the roles of the phase space factors and the invariant amplitude squared. First, we recall that our (on-shell)  $t_n$  amplitudes, being solutions of Eq. 1, are related to the solutions of the original Thompson equation as [5]

$$t_n = \frac{m^2}{E^2} \frac{\hat{t}_n}{(2\pi)^3} . \quad (32)$$

This is just a convenient definition, which makes the relativistic equation formally identical to its non-relativistic counterpart [5]. Applying the same factors to the  $\varphi_n$  amplitudes in Eq. 28, we obtain

$$\varphi_n = \frac{m^2}{4E\pi} \hat{t}_n . \quad (33)$$

Therefore, the Hoshizaki expression, Eq. [30], becomes, in the center-of-mass frame,

$$\frac{d\sigma}{d\Omega} = \frac{m^4}{s(2\pi)^2} (|\hat{a}|^2 + |\hat{m}|^2 + 2(|\hat{c}|^2 + |\hat{g}|^2 + |\hat{h}|^2)) , \quad (34)$$

where  $s$  is the total energy squared, and the ‘‘hat’’ symbol signifies solutions of the relativistic equation, related to the solutions of our ‘‘reduced’’ Thompson equation as in Eq. 32. (As a footnote, we mention that we use natural units,  $\hbar = c = 1$ , throughout this paper. In order to express the differential cross-section in units of  $mb$ , a factor of  $10(\hbar c)^2$  must be applied.)

In our application of the DBHF approach (see Ref. [20] and references therein), one describes the positive energy solutions of the Dirac equation in the medium as

$$u^*(q, \lambda) = \left( \frac{E_q^* + m^*}{2m^*} \right)^{1/2} \begin{pmatrix} \mathbf{1} \\ \frac{\sigma \cdot \vec{q}}{E_q^* + m^*} \end{pmatrix} \chi_\lambda , \quad (35)$$

where the effective mass,  $m^*$ , is defined as  $m^* = m + U_S$ , with  $U_S$  an attractive scalar potential, assumed to be density dependent but momentum independent. Thus, throughout our in-medium calculations, we replace  $m$  with  $m^*$  and  $E = \sqrt{m^2 + q^2}$  with  $E^* = \sqrt{(m^*)^2 + q^2}$ .

Applied to Eq. [34], this yields (consistent with, for instance, Ref. [13])

$$\frac{d\sigma}{d\Omega} = \frac{(m^*)^4}{s^*(2\pi)^2} |\hat{G}|^2, \quad (36)$$

where the ‘‘hat’’ symbol indicates solutions of the (in-medium) Thompson equation.

#### D. Including the Pauli operator

For completeness, we recall that, in analogy with the free-space case, the Bethe-Goldstone equation can be written as [5]

$$\hat{G}^I(\mathbf{q}', \mathbf{q}, \mathbf{P}, k_F) = \hat{V}^I(\mathbf{q}', \mathbf{q}) + \int_{\mathbb{R}^3} \frac{\hat{V}^I(\mathbf{q}', \mathbf{q}'') Q(\mathbf{q}'', \mathbf{P}, k_F) \hat{G}^I(\mathbf{q}'', \mathbf{q}, \mathbf{P}, k_F)}{2(E_q^* - E_{q''}^* + i\epsilon)} d^3 q'', \quad (37)$$

where the asterix signifies in-medium energies and the Pauli operator  $Q$  suppresses scattering into states below the Fermi momentum. More explicitly the Pauli operator for symmetric nuclear matter is defined as

$$Q(\mathbf{q}'', \mathbf{P}, k_F) \equiv \Theta(|\mathbf{P} + \mathbf{q}''| - k_F) \Theta(|\mathbf{P} - \mathbf{q}''| - k_F), \quad (38)$$

where  $\Theta$  is the Heaviside step function,  $\mathbf{P}$  is one half the center of mass momentum,  $\mathbf{P} \pm \mathbf{q}$  are the momenta of the two nucleons in the nuclear matter rest frame, and  $k_F$  is the Fermi momentum, related to the nucleon density by  $\rho = \frac{2k_F^3}{3\pi^2}$ . Clearly, the free-space equation is recovered by using free-space energies and setting  $Q=1$ . The corresponding  $\phi$ -integrated Bethe-Goldstone equation can then be solved in perfect analogy with the free-space case described above.

We also recall that the so called spherical or angle-averaged Pauli operator  $\bar{Q}$  (see Ref. [21] and references therein), is obtained from

$$Q(\mathbf{q}'', \mathbf{P}, k_F) \approx \bar{Q}(q'', P, k_F) = \frac{\int Q(\mathbf{q}'', \mathbf{P}, k_F) d\Omega''}{\int d\Omega''}, \quad (39)$$

unless it's equal to zero or one. Clearly, no angle average is required in our three-dimensional approach.

The case of asymmetric nuclear matter, that is, when two different Fermi momenta,  $k_{F1}$  and  $k_{F2}$ , are present (as would be the case in collisions of two different ions), can be handled by simply modifying the angular integration to implement the restrictions

$$\begin{aligned} |\mathbf{P} + \mathbf{q}''| > k_{F1} \quad \text{and} \quad |\mathbf{P} - \mathbf{q}''| > k_{F2} \implies \\ Q(\mathbf{q}'', \mathbf{P}, k_{F1}, k_{F2}) \equiv \Theta(|\mathbf{P} + \mathbf{q}''| - k_{F1}) \Theta(|\mathbf{P} - \mathbf{q}''| - k_{F2}), \end{aligned} \quad (40)$$

which, again, is easily accomplished in our three-dimensional formalism.

### III. RESULTS AND DISCUSSION

The scattering amplitudes obtained from the solution of the integral equations as described above are the input for calculating NN scattering observables. In this section, we will present and discuss selected *in-medium*  $np$  and  $pp$  cross sections obtained with the exact Pauli operator and compare with previous predictions which utilize the angle-averaged expression. Once again, NN scattering in nuclear matter is not directly measurable, but a model for such process can be indirectly tested through applications in nuclear reactions.

In addition to the elastic differential cross-section, we will also consider polarized scattering, to explore whether the sensitivities we are investigating are more or less pronounced in the spin dependence of the interaction. As a representative example, we have chosen the depolarization parameter,  $D$ , or  $D_{nn}$ .

In Figs. 1-3, we show  $np$  observables at values of the on-shell c.m. momentum corresponding to a free-space incident energy of 50, 100, and 200 MeV, respectively. In each figure, the frames labeled as (a) and (b) display the elastic differential cross-section, whereas those labeled as (c) and (d) show the depolarization parameter.

In all frames, the solid red curve shows the free-space predictions. For the frames on the left-hand side, the dashed blue curve is obtained with the exact Pauli operator, assuming scattering in symmetric nuclear matter with a Fermi momentum of  $1.4 \text{ fm}^{-1}$  [namely, we are solving the Bethe-Goldstone equation with the Pauli operator as in Eq. (38)]; the dotted green curve is the corresponding result with the angle-averaged calculation. For the frames on the right-hand side, we consider scattering in the presence of two different Fermi momenta [see Eq. (40)]. The dashed blue curve and the dotted green one are, again, predictions with the three-dimensional formalism and the angle-averaged approach, respectively.

In all cases, medium effects on the energies are taken into account through the use of nucleon effective masses, which we take from previous calculations [20]. Specifically, the nucleon effective mass in nuclear matter with density corresponding to  $k_F = 1.4 \text{ fm}^{-1}$  is taken to be 612.8 MeV, whereas for  $k_F = 1.1 \text{ fm}^{-1}$  the value is found to be 718.3 MeV.

First, we observe that the density dependence is very large. The differential cross-section is strongly reduced and flattened by medium effects. Also, structures in the spin dependence are heavily suppressed.

Differences between the dashed curve and the dotted one are noticeable, but much smaller than those between the free-space predictions and either one of the medium-modified calculations. Interestingly, those differences are larger for the case of the asymmetric Pauli operator, particularly so in the case of polarized scattering.

We note that the free-space  $np$  cross-section is rather anisotropic, and becomes more so, as energy increases, due to interferences from more partial waves. In the presence of medium effects, the cross-section becomes much more isotropic. Also, medium effects are smaller at the higher energies, as is physically reasonable.

In Figs. 4-6, we provide a similar presentation as the one in Figs. 1-3, but for  $pp$  scattering. As far as general features are concerned, similar considerations apply. Namely, there is strong density dependence, and moderate sensitivity to the use of the angle-dependent Pauli operator. Again, such sensitivity is more pronounced for the cases on the left-hand side.

We note in passing that the free-space  $pp$  differential cross-section is less anisotropic than the  $np$  one, due to the smaller number of partial waves that contribute to it ( $I = 1$  states only), and is symmetric with respect to the  $\theta \rightarrow \pi - \theta$  transformation. In the medium, it is strongly reduced, and, at the higher energies, shows a dramatic change in curvature. Recalling that different partial waves (beyond the  $S$ -waves) contribute non-isotropically to the cross section, we attribute this feature to how the relative role of different partial waves is impacted by the medium.

With regard to sensitivity to the removal of the spherical approximation, we conclude that the latter is slightly more pronounced in the  $np$  case, particularly in the spin-dependent observable. This suggests enhanced sensitivity in the  $I = 0$  channel, which is absent in the  $pp$  interaction.

Overall, we can conclude that small effects from the use of the non-averaged Pauli operator are to be expected in applications involving in-medium NN cross-sections. Highly asymmetric situations (that is, two very unequal Fermi momenta), could be an exception. Furthermore, it is appropriate to point out that the in-medium observables we have shown are obtained from the on-shell G-matrix. At this time, we cannot exclude a larger sensitivity to the removal of the spherical approximation in many-body calculations which utilize the half- or fully-off-shell G-matrix.

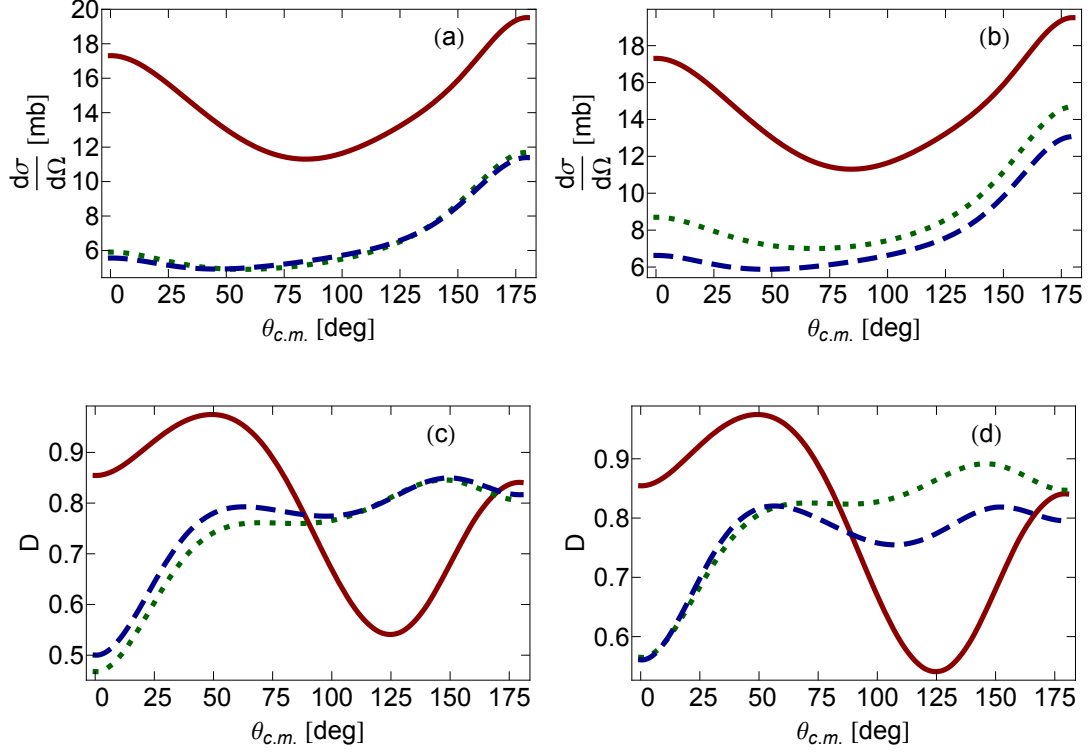


FIG. 1: (Color online) [Figs. (a) and (b)]  $np$  elastic differential cross-section and [Figs. (c) and (d)] depolarization at a laboratory free-space energy of 50 MeV *vs.* the c.m. scattering angle. The solid red curve shows the free-space prediction. The angle-averaged calculation is given by the dotted green curve whereas the dashed blue curve shows the prediction obtained with the exact Pauli operator in symmetric [left side Figs. (a) and (c)] and asymmetric [right side Figs. (b) and (d)] matter at a density equal to  $k_{F_1} = k_{F_2} = 1.4 \text{ fm}^{-1}$  and  $k_{F_1} = 1.1 \text{ fm}^{-1}, k_{F_2} = 1.4 \text{ fm}^{-1}$  respectively.

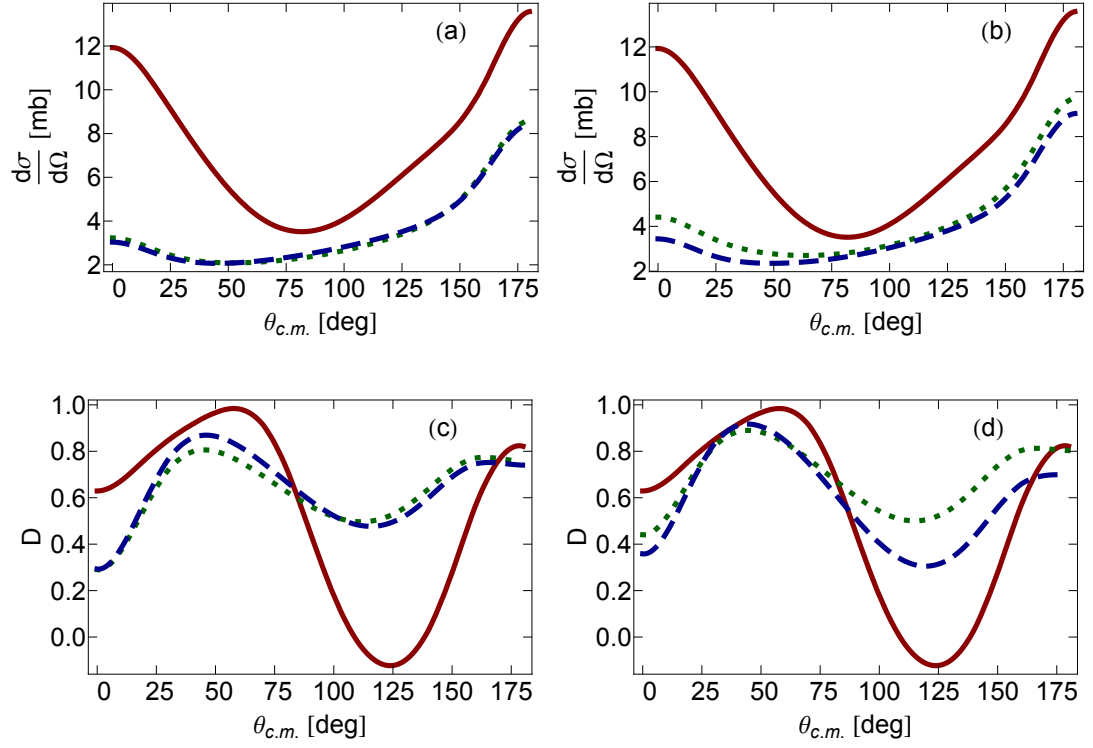


FIG. 2: (Color online) Same as Fig. 1 but at 100 MeV.

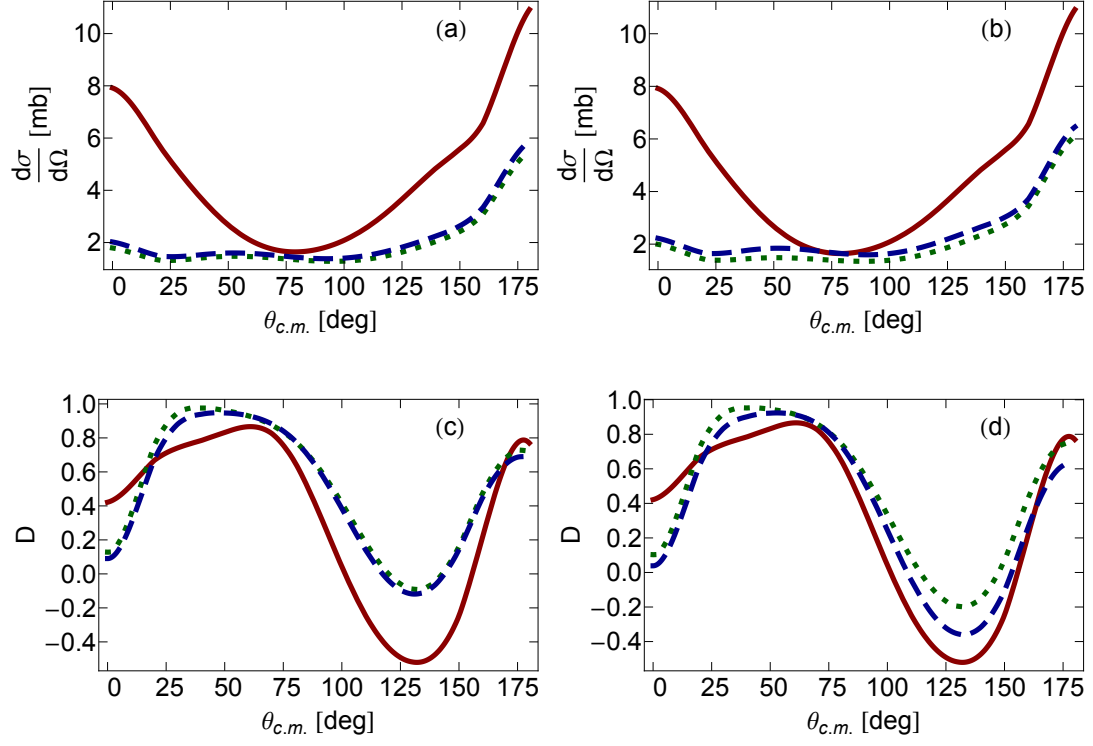


FIG. 3: (Color online) Same as Fig. 1 but at 200 MeV.

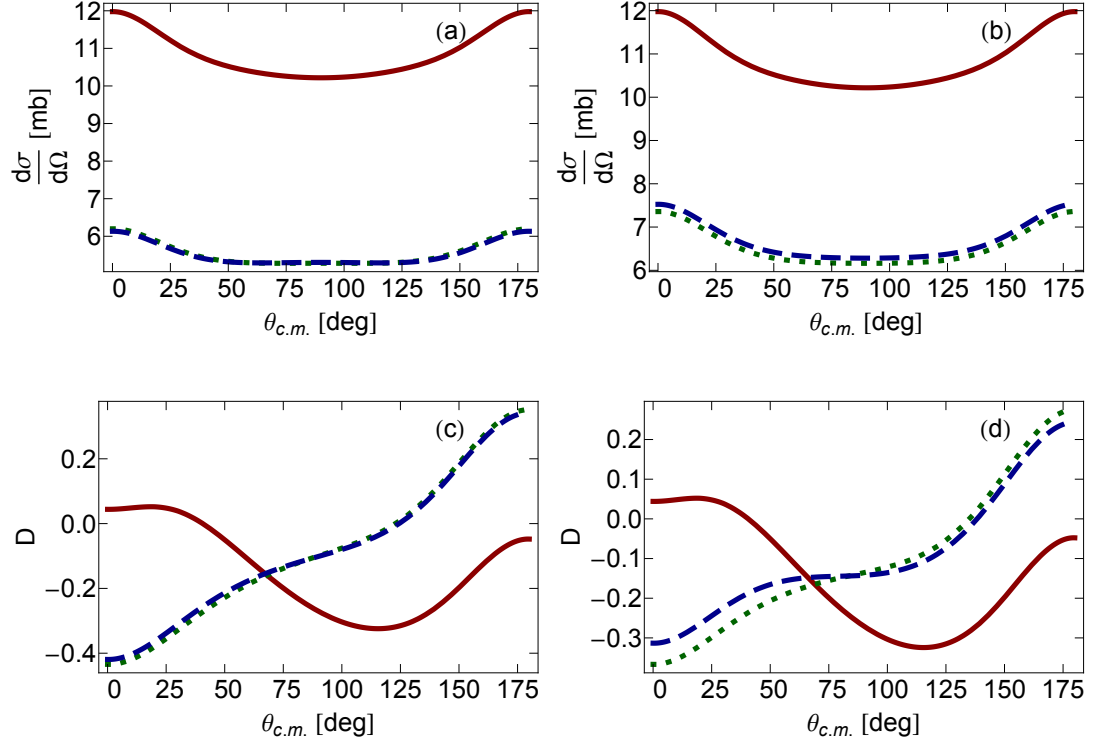


FIG. 4: (Color online) Same as Fig. 1 but for  $pp$  scattering.

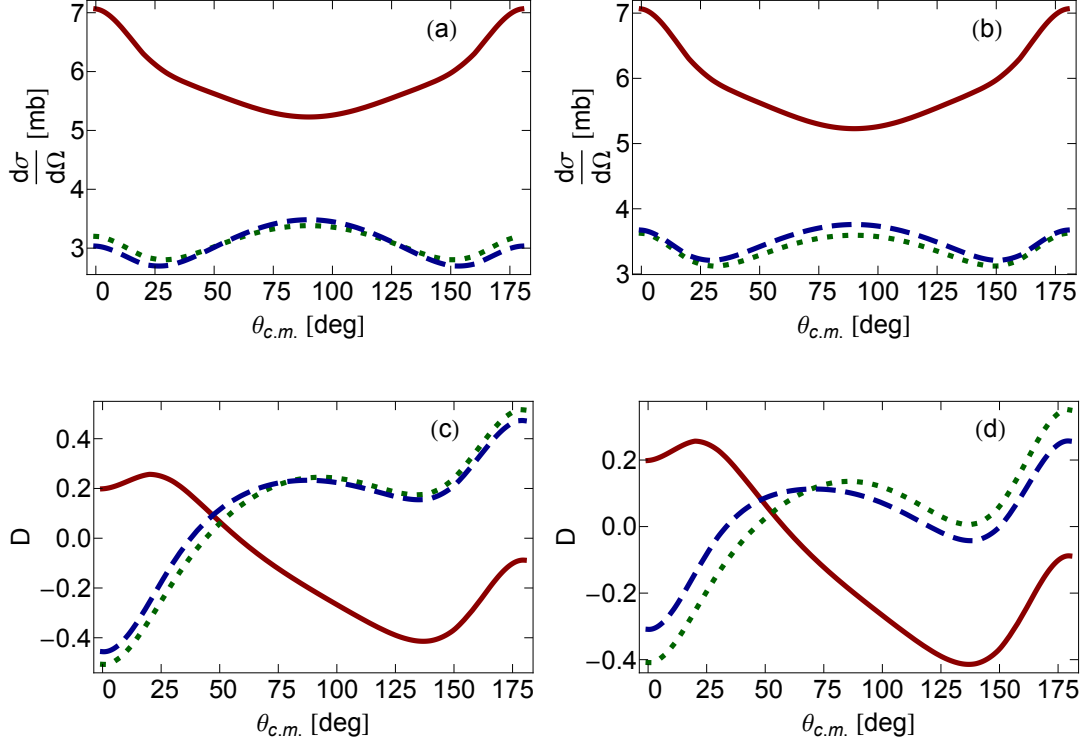


FIG. 5: (Color online) Same as Fig. 4 but at 100 MeV.

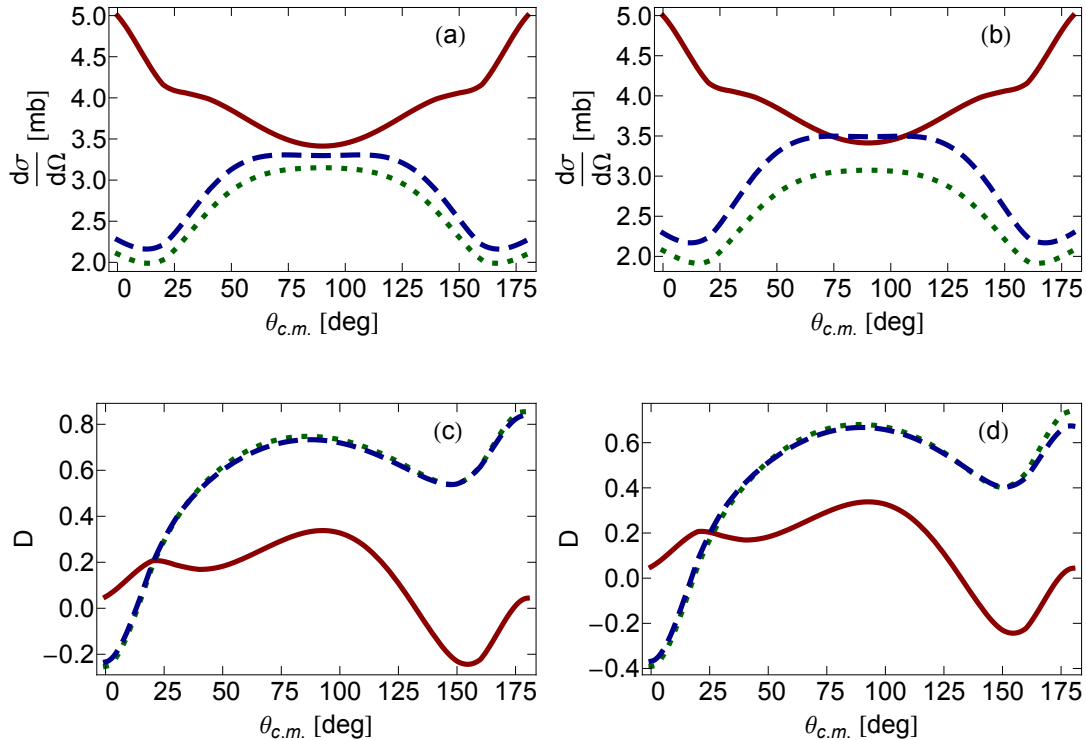


FIG. 6: (Color online) Same as Fig. 4 but at 200 MeV.

#### IV. SUMMARY AND CONCLUSION

We presented an alternative way to solve the Thompson and the Bethe-Goldstone equations in three-dimensional space. The main differences with the solution techniques developed in Sect. II concern the way the azimuthal degree of freedom is integrated out in the equations and how the resulting analytical structure of the equations is handled.

Exact angle-dependent on-shell amplitudes were calculated and used to obtain in-medium NN “observables”. These were compared to partial wave decomposed (angle-independent) solutions which utilized the spherical approximation on the Pauli operator. Only moderate sensitivity was observed between the exact and angle-averaged calculation in this case, although scattering in asymmetric matter (that is, in the presence of two different Fermi momenta), showed enhanced sensitivity.

Finally, Pauli blocking is one of the most important mechanisms governing the scattering of fermions in the many-body system. Regardless the magnitude of the effects we set forth to explore, to the best of our knowledge the solution of the Bethe-Goldstone equation we have presented in this paper is an original one, and has allowed us to better quantify the impact of the historically very popular spherical approximation.

#### ACKNOWLEDGMENTS

Support from the U.S. Department of Energy under Grant No. DE-FG02-03ER41270 is acknowledged.

- 
- [1] K.A. Brueckner, C.A. Levinson, and H.M. Mahmoud, Phys. Rev. **95**, 217 (1954).
  - [2] H. Bethe, Phys. Rev. **103**, 1353 (1956).
  - [3] J. Goldstone, Proc. R. Soc. Lond. A **239**, 267 (1957).
  - [4] H. Bethe, Annu. Rev. Nucl. Sci. **21**, 93 (1971).

- [5] L. White and F. Sammarruca, Phys. Rev. **C88**, 054619 (2013).
- [6] G.F. Bertsch and S. Das Gupta, Phys. Rep. **160**, 189 (1992).
- [7] W. Cassing, W. Metag, U. Mosel, K. Niita, Phys. Rep. **188**, 363 (1990).
- [8] V. R. Pandharipande and S.C. Pieper, Phys. Rev. C **45**, 791 (1992).
- [9] D. Persram and C. Gale, Phys. Rev. C **65**, 064611 (2002).
- [10] Bao-An Li and Lie-Wen Chen, Phys. Rev. C **72**, 064611 (2005).
- [11] G.Q. Li and R. Machleidt, Phys. Rev. C **48**, 1702 (1993).
- [12] G.Q. Li and R. Machleidt, Phys. Rev. C **49**, 566 (1994).
- [13] C. Fuchs, A. Faessler, M. El-Shabshiry, Phys. Rev. C **64**, 024003 (2001).
- [14] R.A. Rice and Y.E. Kim, Few-Body Systems **14**, 127 (1993).
- [15] I. Fachruddin, C. Elster, and W. Glöckle, Phys. Rev. **C62**, 044002 (2000), arXiv:nucl-th/0004057 [nucl-th].
- [16] M. Jacob and G. Wick, Ann. Phys. (N.Y.) **7**, 404 (1959).
- [17] G.E. Brown and A.D. Jackson, *The Nucleon-Nucleon Interaction* (North-Holland, 1976).
- [18] R. Machleidt, K. Holinde, and C. Elster, Phys. Rept. **149**, 1 (1987).
- [19] Norio Hoshizaki, Prog. Theor. Phys. Supplement **42**, 107 (1968).
- [20] F. Sammarruca, Int. J. Mod. Phys. **E19**, 1259 (2010).
- [21] Michael I. Haftel and Frank Tabakin, Nucl. Phys. **A158**, 1 (1970).